ONSET OF PERTURBATIVE QCD REGIME FOR THE PION ELECTROMAGNETIC FORM FACTOR*

I. CAPRINI

Department of Theoretical Physics,
"Horia Hulubei" National Institute for Physics and Nuclear Engineering,
RO-077125, POB-MG6, Măgurele-Bucharest, Romania
E-mail: caprini@theory.nipne.ro

Received February 20, 2013

I investigate the onset of the asymptotic perturbative QCD regime for the pion electromagnetic form factor, using a suitable mathematical technique of analytic continuation from the time-like momenta to space-like momenta. The method leads to almost model-independent upper and lower bounds on the space-like form factor, which exclude the asymptotic perturbative QCD regime for space-like squared momenta less than $7\,\mathrm{GeV}^2$.

PACS: 11.55.Fv, 13.40.Gp, 25.80.Dj.

1. INTRODUCTION

The transition from the soft regime of non-perturbative QCD to the hard regime of perturbative QCD is a complicated, not fully understood problem. In particular, for many exclusive observables the asymptotic behaviour predicted by perturbative QCD is expected to set on rather slowly. A typical example is the pion electromagnetic (vector) form factor $F(t)$, defined through the matrix element

$$\langle\pi^+(p')|J_\mu^{\mathrm{elm}}|\pi^+(p)\rangle = (p+p')_\mu F(t), \qquad t = q^2 = (p'-p)^2. \tag{1}$$

In our notation the space-like axis is defined by $Q^2 = -t > 0$. Near $t = 0$ the form factor is holomorphic and admits the Taylor expansion

$$F(t) = 1 + \frac{1}{6}\langle r_\pi^2\rangle\, t + ct^2 + dt^3 \cdots \tag{2}$$

where $\langle r_\pi^2\rangle$ denotes the charge radius squared.

A unified theoretical treatment of the pion vector form factor does not exist. At low energies its properties are described by Chiral Perturbation Theory (ChPT) [1–3], lattice calculations [4], or various types of QCD sum rules [5, 6]. Perturbative

*Paper presented at "The 8^{th} Workshop on Quantum Field Theory and Hamiltonian Systems", September 19-22, 2012, Craiova, Romania.

QCD can be applied at large momenta on the space-like axis, far from the physical thresholds [7–13]. It has been known since a long time that the non-perturbative and sub-asymptotic terms are non-negligible for this quantity up to relatively high momenta, delaying the onset of the QCD asymptotic regime. Several models have been proposed for the description of the interplay between the soft and the strong dynamics [14–19], but a quantitative estimate of the transition energy from the soft to the hard regime is still missing. The purpose of the present talk is to discuss this problem.

A very rich experimental and theoretical information is now available on the pion vector form factor. However, most of the accurate information regards the behaviour at time-like momenta: the determinations on the space-like axis [20–29] are obtained from indirect experiments and are affected by large uncertainties, especially at high momenta. Therefore, an analytic extrapolation from the time-like to the space-like axis in the momentum plane is necessary. The rigorous properties of analyticity and unitarity play a crucial role in performing this extrapolation.

Causality implies that $F(t)$ is a real analytic function, $F(t^*) = F^*(t)$, in the complex t-plane cut for $t > t_+$, where $t_+ = 4M_\pi^2$ is the lowest unitarity threshold. The discontinuity across the cut is determined by unitarity, which implies in particular that in the elastic region (below the first significant inelastic threshold t_{in}) the spectral function is expressed as

$$\text{Im}F(t+i\epsilon) = \theta(t-t_+)\,\sigma(t) f_1^*(t) F(t), \qquad t_+ \le t \le t_{\text{in}}, \tag{3}$$

where $\sigma(t) = \sqrt{1-t_+/t}$ is the two-particle phase-space and $f_1(t) = \frac{e^{2i\delta_1^1(t)}-1}{2i\sigma(t)}$ is the P-wave of $\pi\pi$ elastic scattering amplitude. For the pion vector form factor the first significant inelastic threshold is at $t_{\text{in}} = (M_\pi + M_\omega)^2 = (0.917\,\text{GeV})^2$. The relation (3) implies the famous Fermi-Watson theorem, which states that in the elastic region the phase of the form factor is equal to the P-wave phase shift $\delta_1^1(t)$ of the $\pi\pi$ elastic scattering:

$$\arg[F(t+i\epsilon)] = \delta_1^1(t), \qquad t_+ \le t \le t_{\text{in}}. \tag{4}$$

Most calculations of the form factor on the space-like axis performed in the past are based on specific parametrizations, which are often extrapolated outside their range of validity, or on dispersive representations, which require an input not fully available. In the present paper the high-energy behaviour of the pion form factor along the space-like axis is investigated by exploiting the information available on the time-like axis in a model-independent formalism, discussed in [30, 31]. The usefulness of this method for improving the knowledge of the pion form factor was demonstrated in [32–34]. In particular, as shown in [33], the method leads to stringent model independent upper and lower bounds on $F(t)$ on the space-like axis, which can be compared with the predictions of perturbative QCD and with specific theoretical models.

After a brief description of the predictions of perturbative QCD in section 2, I review in section 3 the standard types of dispersion relations applied in the past to the pion form factor, and express the present experimental and theoretical input on the function $F(t)$ as an extremal problem on a class of analytic functions. The solution of this problem is given in section 4 and is applied in section 5 for deriving upper and lower bounds on the form factor at space-like intermediate momenta. The implications of the results for the onset of the perturbative QCD regime are briefly discussed in the final section 6.

2. PERTURBATIVE QCD

The high-energy behaviour along the space-like axis of the pion electromagnetic form factor is predicted by the factorization theorem for exclusive quantities in perturbative QCD [7–10]: the relevant hadronic quantity is expressed as a convolution of a partonic kernel and the distribution amplitudes describing the probability of the constituent quarks to carry a certain fraction of the hadron momentum.

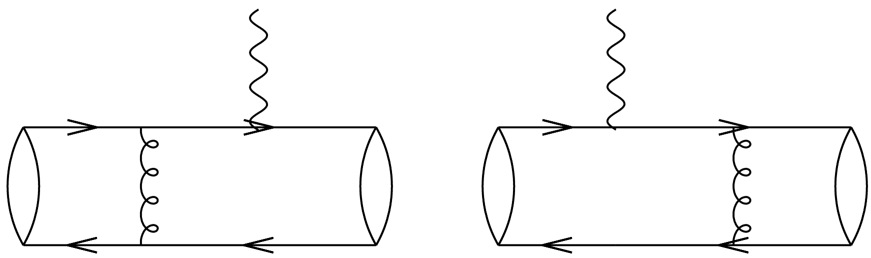

Fig. 1 – Feynman graphs for the calculation of the pion electromagnetic form factor in perturbative QCD to LO. The solid lines denote the quarks and anti-quarks, the curly lines the gluons and the wavy lines the photons. The blobs denote the distribution functions of the quarks in the pion.

For the pion electromagnetic form factor the leading order (LO) Feynman diagrams shown in Fig. 1 give the contribution

$$F_{\rm pert}^{\rm LO}(-Q^2) = \frac{8\pi f_\pi^2 \alpha_s(\mu^2)}{Q^2}, \tag{5}$$

where $f_\pi = 130.4\,{\rm MeV}$ is the pion decay constant and $\alpha_s(\mu^2)$ the strong coupling at the renormalization scale μ, fixed usually by the choice $\mu^2 = Q^2$. Next-to-leading order (NLO) perturbative corrections have been calculated in [11–13], using various renormalization schemes and pion distribution amplitudes (DA). In particular, the result in the $\overline{\rm MS}$-renormalization scheme with asymptotic DA reads [12]

$$F_{\rm pert}^{\rm NLO}(-Q^2) = \frac{8 f_\pi^2 \alpha_s^2(\mu^2)}{Q^2}\left[\frac{\beta_0}{4}\left(\ln\frac{\mu^2}{Q^2}+\frac{14}{3}\right)-3.92\right], \tag{6}$$

where $\beta_0 = 11 - 2n_f/3$ is the first coefficient in the perturbative expansion of the renormalization group β-function, n_f being the number of active quark flavours. The ambiguities that affect the perturbative QCD predictions have been investigated in many papers, where in particular the dependence on the renormalization scale and various prescriptions for scale setting have been discussed [12, 14].

It is currently accepted that perturbative QCD is valid for hard momentum transfers, *i.e.* at large values of Q^2, far from the thresholds of hadronic production, where the running strong coupling $\alpha_s(Q^2)$ is small due to the asymptotic freedom of QCD. However, the practical question as to where precisely starts the perturbative regime does not have a simple answer, due to the lack of accurate data at large energies on the space-like axis: as mentioned above, these data are obtained indirectly and are affected by large errors. Therefore, the analytic continuation of the form factor from the time-like axis to the space-like axis in the complex t-plane is necessary.

3. ANALYTIC CONTINUATION

There are three known types of integral representations allowing this analytic continuation: the standard dispersion relation, based on Cauchy integral and the reality property, written (modulo subtractions) as

$$F(t) = \frac{1}{\pi} \int_{t_+}^{\infty} \frac{\mathrm{Im} F(t' + i\epsilon) dt'}{t' - t}, \tag{7}$$

the Omnès representation, which expresses the function in terms of its phase

$$F(t) = P(t) \exp\left(\frac{t}{\pi} \int_{t_+}^{\infty} dt' \frac{\delta(t')}{t'(t'-t)} \right), \qquad \delta(t) \equiv \arg F(t + i\epsilon), \tag{8}$$

where $P(t)$ is an arbitrary polynomial accounting for the zeros of $F(t)$ at points t_i in the complex plane, $P(t_i) = 0$, and the representation in terms of the modulus

$$F(t) = B(t) \exp\left(\frac{\sqrt{t_+ - t}}{\pi} \int_{t_+}^{\infty} \frac{\ln |F(t')| \, \mathrm{d}t'}{\sqrt{t' - t_+}(t' - t)} \right), \tag{9}$$

where $B(t)$ is a so-called Blaschke factor, with the property $|B(t)| = 1$ for $t > t_+$, which also accounts for the possible zeros of the form factor at points t_i, $B(t_i) = 0$.

None of these standard representations has complete input: the dispersion relation (7) involves the imaginary part, which is not directly measurable. The phase $\delta(t)$ required in (8) is known from Fermi-Watson theorem (4) and the P wave phase shift of $\pi\pi$ scattering only in the elastic region $t < t_{\text{in}}$, while the modulus $|F(t)|$ required in (9) is measured now experimentally with increased precision by several experiments, for instance by BaBar Collaboration [38], but is however poorly known at low energies and above 3 GeV. Moreover, both the phase and modulus representations require the positions of the zeros in the complex plane, which are not known.

In the present talk, I shall make conservative use of the available information on the form factor. The first input is provided by Fermi-Watson theorem (4), with the phase shift $\delta_1^1(t)$ for $t \le t_{\rm in}$ calculated with high precision by using ChPT and dispersive (Roy) equations for $\pi\pi$ amplitude [35–37]. The second ingredient is provided by the data on the modulus $|F(t)|$ above $t_{\rm in}$, measured from the $e^+e^- \to \pi^+\pi^-$ annihilation (in particular, the data available up to 3 GeV from the BaBar experiment [38]). These data allow a good estimate of the integral

$$\frac{1}{\pi}\int_{t_{\rm in}}^{\infty} \rho(t)|F(t)|^2 dt = I, \tag{10}$$

for a class of weight functions $\rho(t)$, discussed in [32–34]. In particular, a suitable choice for the present problem is $\rho(t) = 1/\sqrt{t}$, for which the quantity I, evaluated with the data from [38] up to 3 GeV and conservative assumptions above this energy, is

$$I = 0.687 \pm 0.028. \tag{11}$$

An additional input is the normalization $F(0) = 1$ displayed in the Taylor expansion (2), and the range

$$\langle r_\pi^2 \rangle = 0.43 \pm 0.01\,{\rm fm}^2, \tag{12}$$

for the charge radius, suggested from studies based on ChPT [3]. The formalism allows in fact the inclusion of an arbitrary number of derivatives at $t = 0$. It allows also the inclusion of an arbitrary number of values at points below the unitarity threshold:

$$F(t_n) = F_n \pm \epsilon_n, \qquad t_n < t_+, \qquad n = 1,2,\ldots N, \tag{13}$$

where F_n and ϵ_n represent the central value and the uncertainty. In particular, it is convenient to include the input value

$$F(-2.45\,{\rm GeV}^2) = 0.167 \pm 0.010^{+0.013}_{-0.007}, \tag{14}$$

known from the recent precise measurements of the $ep \to en\pi^+$ process [28, 29].

In the next section, I shall show how to exploit in an optimal way the input described above for finding model-independent upper and lower bounds on the form factor $F(t)$ in the space-like region $t < 0$.

4. SOLUTION OF THE EXTREMAL PROBLEM

The problem formulated in the previous section belongs to the so-called Meiman class of extremal problems and can be solved using standard mathematical methods, discussed in detail in [30, 31]. One defines first the Omnès function

$$\mathcal{O}(t) = \exp\left(\frac{t}{\pi}\int_{4M_\pi^2}^{\infty} dt' \frac{\delta(t')}{t'(t'-t)}\right), \tag{15}$$

where $\delta(t) = \delta_1^1(t)$ for $t \leq t_{\rm in}$, and is an arbitrary function, sufficiently smooth (*i.e.* Lipschitz continuous) for $t > t_{\rm in}$. As shown in [31], the results do not depend on the choice of the function $\delta(t)$ for $t > t_{\rm in}$. The crucial remark is that the function $h(t)$ defined by

$$F(t) = \mathcal{O}(t)h(t) \tag{16}$$

is analytic in the t-plane cut only for $t > t_{\rm in}$. Furthermore, equality (10) implies that $h(t)$ satisfies the condition

$$\frac{1}{\pi}\int_{t_{\rm in}}^{\infty} dt\, \rho(t)|\mathcal{O}(t)|^2|h(t)|^2 = I. \tag{17}$$

This relation can be written in a canonical form by performing the conformal transformation

$$\tilde{z}(t) = \frac{\sqrt{t_{\rm in}} - \sqrt{t_{\rm in} - t}}{\sqrt{t_{\rm in}} + \sqrt{t_{\rm in} - t}}, \tag{18}$$

which maps the complex t-plane cut for $t > t_{\rm in}$ onto the unit disk $|z| < 1$ in the z-plane defined by $z \equiv \tilde{z}(t)$, and defining a function $g(z)$ by

$$g(z) = w(z)\,\omega(z)\,F(\tilde{t}(z))\,[\mathcal{O}(\tilde{t}(z))]^{-1}, \tag{19}$$

where $\tilde{t}(z)$ is the inverse of $z = \tilde{z}(t)$, for $\tilde{z}(t)$ as defined in (18), and $w(z)$ and $\omega(z)$ are calculable outer functions, *i.e.* functions analytic and without zeros for $|z| < 1$, defined in terms of their modulus on the boundary, related to $\sqrt{\rho(t)}$ and $|\mathcal{O}(t)|$, respectively. They can be written as [30, 31, 33]

$$w(z) = (2\sqrt{t_{\rm in}})^{1/2}\,\frac{(1-z)^{1/2}}{(1+z)}, \tag{20}$$

$$\omega(z) = \exp\left(\frac{\sqrt{t_{\rm in} - \tilde{t}(z)}}{\pi}\int_{t_{\rm in}}^{\infty} \frac{\ln|\mathcal{O}(t')|\,{\rm d}t'}{\sqrt{t' - t_{\rm in}}(t' - \tilde{t}(z))}\right). \tag{21}$$

From (16) it follows that the product $F(\tilde{t}(z))\,[\mathcal{O}(\tilde{t}(z))]^{-1}$ appearing in (19) is equal to the function $h(\tilde{t}(z))$, which is analytic in $|z| < 1$. Therefore, the function $g(z)$ defined in (19) is analytic in $|z| < 1$. Moreover, using the definition of the functions $w(z)$ and $\omega(z)$, it is easy to see that the equality (17) can be written in terms of $g(z)$ as

$$\frac{1}{2\pi}\int_0^{2\pi} {\rm d}\theta |g(\zeta)|^2 = I, \qquad \zeta = {\rm e}^{i\theta}. \tag{22}$$

The transformation (18) maps the origin $t = 0$ of the t-plane onto the origin $z = 0$ of the z-plane. From (19) it follows that each coefficient $g_k \in R$ of the expansion

$$g(z) = g_0 + g_1 z + g_2 z^2 + g_3 z^3 + \dots \tag{23}$$

is expressed in terms of the coefficients of order lower or equal to k, of the Taylor series expansion of the form factor. Furthermore, the values $F(t_n)$ of the form factor at a set of real points $t_n < t_+$, $n = 1, 2, ...N$ are related to the values $g(z_n)$ at $z_n = \tilde{z}(t_n)$ by

$$g(z_n) = w(z_n)\,\omega(z_n)\,F(t_n)\,[\mathcal{O}(t_n)]^{-1}. \tag{24}$$

Then the L^2 norm condition (22) implies the determinantal inequality (for a proof and older references see [31]):

$$\begin{vmatrix} \bar{I} & \bar{\xi}_1 & \bar{\xi}_2 & \cdots & \bar{\xi}_N \\ \bar{\xi}_1 & \dfrac{z_1^{2K}}{1-z_1^2} & \dfrac{(z_1 z_2)^K}{1-z_1 z_2} & \cdots & \dfrac{(z_1 z_N)^K}{1-z_1 z_N} \\ \vdots & \vdots & \vdots & \vdots & \vdots \\ \bar{\xi}_N & \dfrac{(z_1 z_N)^K}{1-z_1 z_N} & \dfrac{(z_2 z_N)^K}{1-z_2 z_N} & \cdots & \dfrac{z_N^{2K}}{1-z_N^2} \end{vmatrix} \geq 0, \tag{25}$$

where $\bar{I} = I - \sum_{k=0}^{K-1} g_k^2$ and $\bar{\xi}_n = g(z_n) - \sum_{k=0}^{K-1} g_k z_n^k$.

The inequality (25) leads to rigorous upper and lower bounds on the value of the form factor at one space-like point $t < 0$ using input values at other points inside the holomorphy domain or the derivatives at $t = 0$. The calculation amounts to solving simple quadratic equations for the quantities $g(z_n)$, related to the values $F(t_n)$ of the form factor through the relation (24).

5. BOUNDS ON THE SPACE-LIKE FORM FACTOR

Fig. 2 shows the upper and lower bounds on the product $Q^2 F(-Q^2)$ in the range $0 \leq Q^2 \leq 10\,\mathrm{GeV}^2$, obtained with the weight $\rho(t) = 1/\sqrt{t}$ in the integral condition (10) and the input defined by the normalization $F(0) = 1$ and the relations (4), (11), (12) and (14). The Omnès function (15) was calculated using below $t_{\rm in}$ the phase shift $\delta_1^1(t)$ obtained with great precision from Roy equations for the $\pi\pi$ amplitude [35–37], and above $t_{\rm in}$ an arbitrary smooth continuation of this phase approaching π at large t. As mentioned above, in [31] it was shown that the bounds are independent of the particular form of the phase above $t_{\rm in}$, and this property was checked numerically with great precision.

The inner white region is the allowed domain delimited by the upper and lower bounds obtained with the central values of the input parameters, while the cyan bands show the enlarged allowed domain obtained with the inclusion of the errors of the input. At each point the error is obtained by varying simultaneously the input quantities and taking the most conservative bounds. A significant contribution to the size of the cyan domain is brought by the experimental uncertainty of the space-like input (14).

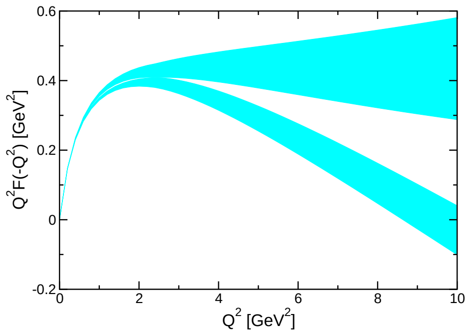

Fig. 2 – Upper and lower bounds on the product $Q^2F(-Q^2)$ derived with the weight $\rho(t) = 1/\sqrt{t}$ by including the charge radius (12) and the space-like datum (14). The inner white region denotes the allowed domain delimited by the upper and lower bounds obtained with the central values of the input; the cyan bands show the enlarged allowed domain, delimited by the upper and lower bounds obtained by varying the input quantities inside their error intervals.

In Figs. 3 the allowed range of $Q^2\,F(-Q^2)$ as a function of Q^2 is confronted with some of the data available from experiments [20–29]. At low Q^2, most of the low energy data are consistent with the narrow allowed band predicted by the present analysis. The most recent data from [28, 29] are well accommodated within the allowed band, which is not surprising as one of these points was used as input. There are however some inconsistencies between the allowed domain derived here and the data reported in Refs. [21], [22] and [24], in spite of their large errors.

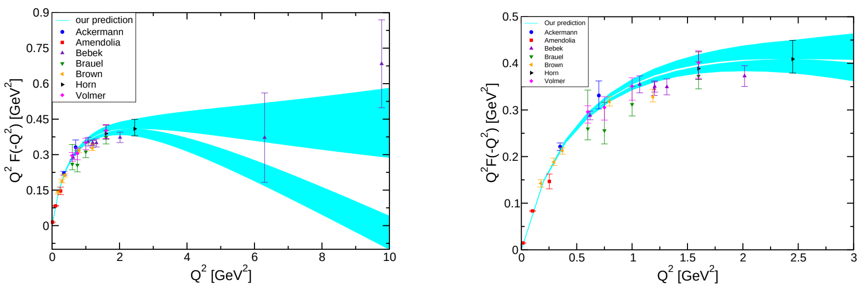

Fig. 3 – Comparison of the bounds with several sets of experimental data. Left: all data; right: enlarged view of the low-energy region.

Finally, in Fig. 4 the allowed domain is compared with the predictions of perturbative QCD and several non-perturbative models proposed in the literature for the space-like form factor at intermediate energies [6, 15–19]. In the LO expression (5), we have taken the scale $\mu^2 = Q^2$ and used the running coupling to one loop, $\alpha_s(Q^2) = 4\pi/(\beta_0 \ln(Q^2/\Lambda^2))$, with $n_f = 3$ active flavours and $\Lambda = 0.214$ GeV, which gives $\alpha_s(M_\tau^2) = 0.33$, the average of the most precise recent predictions from hadronic τ decays [39].

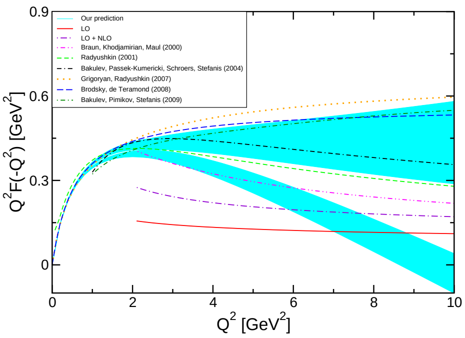

Fig. 4 – Comparison of the bounds with perturbative QCD and several non-perturbative models.

6. DISCUSSION AND CONCLUSIONS

For testing perturbative QCD in the case of exclusive quantities, the analytic continuation from the time-like axis to the space-like axis in the energy plane is often required. In this talk I showed that the phase of the pion form factor along the elastic part of the unitarity cut, together with a conservative estimate of an integral involving the square of the modulus on the complementary part of the cut, exploited by a suitable mathematical formalism, lead to rather stringent upper and lower bounds on $F(t)$ at intermediate space-like energies.

The bounds derived in this formalism are almost model-independent and very robust, allowing to make definite statements about the onset of perturbative QCD. From Fig. 4 one can see that perturbative QCD to LO is excluded for $Q^2 < 7\,\text{GeV}^2$, and perturbative QCD to NLO is excluded for $Q^2 < 6\,\text{GeV}^2$, respectively. If we restrict to the inner white allowed domain obtained with the central values of the input, the exclusion regions become $Q^2 < 9\,\text{GeV}^2$ and $Q^2 < 8\,\text{GeV}^2$, respectively. Among the theoretical models, the light-cone QCD sum rules [6] and the local quark-hadron duality model [15] are consistent with the allowed domain derived here for a large energy interval, while the remaining models are consistent with the bounds at low energies, but seem to predict too high values at higher Q^2. Stronger statements about the onset of perturbative QCD for the pion electromagnetic form factor will be possible by implementing in the present formalism more accurate experimental data at a few space-like points, expected to be available in the near future.

Acknowledgments. This talk is based on works done in collaboration with B. Ananthanarayan and I.Sentitemsu Imsong from the Centre for High Energy Physics, Indian Institute of Science, Bangalore, India. Support from CNCS in the Program Idei - PCE, Contract No. 121/2011 is acknowledged.

REFERENCES

1. J. Bijnens, G. Colangelo, P. Talavera, JHEP **9805**, 014 (1998).
2. H. Leutwyler, "*Electromagnetic form factor of the pion*", `arXiv:hep-ph/0212324` (2002).
3. G. Colangelo, Nucl. Phys. Proc. Suppl. **131**, 185 (2004).
4. S. Aoki *et al.* [JLQCD and TWQCD Collaborations], Phys. Rev. D **80**, 034508 (2009).
5. V.M. Braun, I.E. Halperin, Phys. Lett. B **328**, 457 (1994).
6. V.M. Braun, A. Khodjamirian, M. Maul, Phys. Rev. D **61**, 073004 (2000).
7. G.R. Farrar, D.R. Jackson, Phys. Rev. Lett. **43**, 246 (1979).
8. G.P. Lepage, S.J. Brodsky, Phys. Lett. B **87**, 359 (1979).
9. A.V. Efremov, A.V. Radyushkin, Phys. Lett. B **94**, 245 (1980).
10. V.L. Chernyak, A.R. Zhitnitsky, V.G. Serbo, JETP Lett. **26**, 594 (1977) [Pisma Zh. Eksp. Teor.Fiz. **26**, 760–763 (1977)].
11. B. Melic, B. Nizic, K. Passek, Phys. Rev. D **60**, 074004 (1999).
12. B. Melic, B. Nizic, K. Passek, "*On the PQCD prediction for the pion form factor*", `arXiv:hep-ph/9908510` (2009).
13. Hsiang-nan Li, Yue-Long Shen, Yu-Ming Wang, Hao Zou, Phys. Rev. D **83**, 054029 (2011).
14. S.J. Brodsky, C.-R. Ji, A. Pang, D.G. Robertson, Phys. Rev. D **57**, 245 (1998).
15. A.V. Radyushkin, "*QCD Calculations of Pion Electromagnetic and Transition Form Factors*", `arXiv:hep-ph/0106058` (2001).
16. A.P. Bakulev, K. Passek-Kumericki, W. Schroers, N.G. Stefanis, Phys. Rev. D **70**, 033014 (2004).
17. A.P. Bakulev, A.V. Pimikov, N.G. Stefanis, Phys. Rev. D **79**, 093010 (2009).
18. H.R. Grigoryan, A.V. Radyushkin, Phys.Rev. D **76**, 115007 (2007).
19. S.J. Brodsky, G.F. de Teramond, Phys. Rev. D **77**, 056007 (2008).
20. C.N. Brown *et al.*, Phys. Rev. D **8**, 92 (1973).
21. C.J. Bebek *et al.*, Phys. Rev. D **9**, 1229 (1974); Phys. Rev. D **13**, 25 (1976).
22. H. Ackermann *et al.*, Nucl. Phys. B **137**, 294 (1978).
23. C.J. Bebek *et al.*, Phys. Rev. D **17**, 1693 (1978).
24. P. Brauel *et al.*, Z. Phys. C **3**, 101 (1979).
25. S.R. Amendolia *et al.* [NA7 Collaboration], Nucl. Phys. B **277**, 168 (1986).
26. J. Volmer *et al.* [The Jefferson Lab F(pi) Collaboration], Phys. Rev. Lett. **86**, 1713 (2001).
27. V. Tadevosyan *et al.* [Jefferson Lab F(pi) Collaboration], Phys. Rev. C **75**, 055205 (2007).
28. T. Horn *et al.* [Jefferson Lab F(pi)-2 Collaboration], Phys. Rev. Lett. **97**, 192001 (2006).
29. G. M. Huber *et al.* [Jefferson Lab Collaboration], Phys. Rev. C **78**, 045203 (2008).
30. I. Caprini, Eur. Phys. J. C **13**, 471 (2000).
31. G. Abbas, B. Ananthanarayan, I. Caprini, I.S. Imsong, S. Ramanan, Eur. Phys. J. A **45**, 389 (2010).
32. B. Ananthanarayan, I. Caprini, I.S. Imsong, Phys. Rev. D **83**, 096002 (2011).
33. B. Ananthanarayan, I. Caprini, I.S. Imsong, Phys. Rev. D **85**, 096006 (2012).

34. B. Ananthanarayan, I. Caprini, D. Das, I.S. Imsong, Eur. Phys. J. C **72**, 2192 (2012).
35. B. Ananthanarayan, G. Colangelo, J. Gasser, H. Leutwyler, Phys. Rept. **353**, 207 (2001).
36. R. Garcia-Martin, R. Kaminski, J.R. Pelaez, J. Ruiz de Elvira, F.J. Yndurain, Phys. Rev. D **83**, 074004 (2011).
37. I. Caprini, G. Colangelo, H. Leutwyler, Eur. Phys. J. C **72**, 1860 (2012).
38. B. Aubert *et al.* [BABAR Collaboration], Phys. Rev. Lett. **103**, 231801 (2009).
39. J. Beringer *et al.* (Particle Data Group), Phys. Rev. D **86**, 010001 (2012).